Bioactive Materials 17 (2022) 248–260

Contents lists available at ScienceDirect

Bioactive Materials

journal homepage: www.keaipublishing.com/en/journals/bioactive-materials

A self-crosslinking, double-functional group modified bacterial cellulose gel used for antibacterial and healing of infected wound

Yajie Xie [a,1], Kun Qiao [a,1], Lina Yue [b,1], Tao Tang [c], Yudong Zheng [a,*], Shihui Zhu [c,**], Huiyi Yang [a], Ziyuan Fang [a]

[a] School of Material Science and Engineering, University of Science and Technology Beijing, Beijing, China
[b] Hebei Key Laboratory of Hazardous Chemicals Safety and Control Technology, School of Chemical and Environmental Engineering, North China Institute of Science and Technology, Langfang, 065201, Hebei, China
[c] Department of Burn Surgery, The First Affiliated Hospital of Naval Medical University, Shanghai, 200433, China

ARTICLE INFO

Keywords:
Self-crosslinking
Bacterial cellulose
Cell migration
Wound healing
Antimicrobial properties

ABSTRACT

Cellulose/chitosan composite, as a mature commercial antibacterial dressing, is an important type of wound repair material. However, how to achieve the perfect compound of two components and improve antibacterial activity is a major, lingering issue. In this study, a bifunctional group modified bacterial cellulose (DCBC) was prepared by carboxymethylation and selective oxidation. Further, the chitosan (CS) was compounded in the network of DCBC by self-crosslinking to form dialdehyde carboxymethyl bacterial cellulose/chitosan composites (S-DCBC/CS). The aldehyde group can react with amino of CS by Schiff base reaction. The carboxyl group of DCBC and the amorphous distribution of CS molecular chains increase the antimicrobial properties of composites. The bacteriostatic rate of composites could be higher than 95%. Bacteria can be attracted onto the surface of composites, what we call it "directional adhesion antibacterial effects". In particular, a kind of large animal wound model, deep II degree infected scald of Bama miniature pig, was used to research the antimicrobial and healing properties of materials. The S-DCBC/CS can effectively inhibit bacterial proliferation of wound and kill the bacteria. The wound healing rate of S-DCBC/CS was up to 80% after three weeks. The composites show better antibacterial and promoting concrescence effects than traditional chitosan dressings.

1. Introduction

Wound healing is a multifactorial, physiological and complicated process and generally needs to be covered with a dressing immediately after skin was damaged, because complications associated with wounds are infection, deformity, overgrowth of scar tissue and bleeding [1,2]. However, the traditional dressing is not able to meet the demands which are antibacterial activity, breathability and liquid absorption, especially the moisture retention. Most of them are not functional in wound healing. Besides that, the wet healing theory has set new requirements to new designed wound dressing which include hydrogel dressings, cellulose dressing, chitosan dressing and alginate medical dressings. An ideal material for wound dressing should have some advantages, such as high absorbing ability [3], good oxygen permeability, pain alleviation, easy removal, infection inhibition, wound healing promotion, and reduced scarring [4,5].

Bacterial cellulose (BC), produced by *Acetobacter xylinum* and other genera and the cell-free enzyme systems [6], is becoming a promising biopolymer for several applications, including optically transparent nanocomposites [7,8], food additives [9], textile materials [10] and biomedical materials [11,12], due to its unique properties, such as high mechanical strength, high crystallinity and a highly pure nanofibrillar network structure [13]. Biomedical applications of BC have received considerable attention in literature, for example, in wound dressing [14], blood vessels, vascular grafts [15] and delivery systems of drug and protein [16,17]. In particular, BC has attracted a host of research interests in skin tissue repair and wound care materials, which closely mimics collagen [18]. Although BC has been shown to be effective as

Peer review under responsibility of KeAi Communications Co., Ltd.
* Corresponding author.
** Corresponding author.
E-mail addresses: zhengyudong@mater.ustb.edu.cn (Y. Zheng), doctorzhushihui@163.com (S. Zhu).
[1] Yajie Xie, Kun Qiao and Lina Yue contributed equally to this work and should be considered as co-first authors.

https://doi.org/10.1016/j.bioactmat.2022.01.018
Received 31 October 2021; Received in revised form 8 January 2022; Accepted 10 January 2022
Available online 19 January 2022

wound dressing, it has no antimicrobial properties and promoting healing capability by itself to prevent the wound infection [18]. In order to overcome this shortcoming, fabrication of composite blends with other natural biopolymers [19,20] or nanoparticles [21,22] have been suggested [23]. Wu et al. first used in-situ reduction to obtain the BC/nano-Ag antibacterial dressing which had good antibacterial effects. But the biosafety of nano-Ag is still debatable in recent years. Other inorganic nanoparticles, including ZnO, TiO_2, and Cu, has the similar question. Other researchers use the organic antibacterial agent, such as quaternary ammonium compounds (QACs), metformin and chitosan (CS).

Chitosan, as effective antibacterial ingredients, have been widely used in dressing [24,25], because of its nontoxic, biocompatible, antimicrobial activity [26], biodegradable, moisture retentive and readily available properties [27] and a large number of derivatives also have been described [28]. The antimicrobial activity of CS is attributed to the large number of amino in CS molecular. Therefore, CS/BC composites can potentially be a promising candidate for wound dressing [29,30] as well as for food packaging [31]. In earlier research, BC/CS composite has been successfully prepared by immersing wet BC pellicle in CS solution followed by freeze-drying process. The mechanical properties of BC/CS composite are maintained at certain levels between BC and CS [32,33]. In order to improve the mechanical properties, the Zhong group prepared a novel BC/CS semi-interpenetrating network hydrogels *via* blending the slurry of BC with CS solution followed by cross-linking with glutaraldehyde. The hydrogels showed antibacterial activity against tested Gram-positive and Gram-negative bacteria [34]. In addition to using glutaraldehyde as a crosslinking agent, acrylic acid also is used for crosslinking between BC and CS [35].

According to recent literature, most of the studies deal only with the preparation of BC/CS mixed materials through the following two methods. One method is dipping BC into an acetic acid solution of chitosan [36] and then freeze-drying [37]. The second way is adding the crosslinking agent. There are some other methods including irradiation crosslinking [38], the addition of CS into the culture medium [39]. However, all of these methods have their disadvantages respectively, for example, poor mechanical properties, the toxicity of crosslinking agent and complicated synthesis process which involves irradiation control, cleaning small molecule and control of culture conditions and so on. Therefore, a new method is used for preparing BC/CS composites. Inspired by the oxidation modified cotton cellulose as a crosslinking medium and Schiff's base reaction between amine and aldehyde, Wang [40] prepared a kind of BC/CS composites that could be used in soft tissue reconstructions by the self-crosslinking reaction. In this reaction, the oxidized BC is both matrix material and crosslinking ingredient. The using of toxic cross-linker can be avoided in order to ensure the biocompatibility. However, it is worth noting that the antimicrobial properties may be reduce because of the consumption of amine in this reaction. Thus, how to balance crosslinking and antimicrobial is an important problem in preparation BC/CS composites by self-crosslinking.

Hence, a bifunctional group modified BC which included aldehyde group and carboxymethyl was designed and prepared by substitution reaction and selective oxidation successfully. This modified BC could cross-link with chitosan to form stable composites by Schiff base reaction between aldehyde group and amino. The carboxymethyl group of BC molecule and the amorphous distribution of the CS molecular chains enhance the antibacterial activity of this composites. The microfluidic chip technology and immunofluorescence staining are used for researching cell proliferation, cell migration and collagen I expression. What is more, the directional adhesion and antibacterial effects of composites against different bacteria as well as action mechanisms were investigated. In particular, the composites as a wound dressing were used for treating deep II degree scald wounds in Bama miniature pig. To test the antibacterial ability of the S-DCBC/CS (self-crosslinking dialdehyde carboxymethyl bacterial cellulose/chitosan) composites, the wounds were infected by seeding bacteria. These DCBC/CS composites is a good kind of antimicrobial materials that would be utilized for infectious wound as a wound dressing.

2. Materials and methods

2.1. Materials

Bacterial cellulose (BC) was offered by Hainan Yida Food Co., Ltd. Chitosan (CS, the viscosity is 300 mPa s) was purchased from Weifang sea source Biological Products Co., Ltd. Sodium periodate ($NaIO_4$), hydrochloric acid (HCl), Sodium chloroacetate ($ClCH_2COONa$) and sodium hydroxide (NaOH) were purchased from Sinopharm Chemical Reagent Beijing Co., Ltd.

2.2. Preparation of the dialdehyde carboxymethyl bacterial cellulose (DCBC)

The preprocessing method of pure BC is the same as that of previous research [41]. The carboxymethyl bacterial cellulose (CBC) was prepared as follows. Firstly, BC was dissolved in a mixed solution with deionized water and ethyl alcohol (The volume ratio of H_2O and ethyl alcohol is 3:4) in order to exchange the solvent. Then BC was immersed into the aqueous sodium hydroxide (10%) over 40 min at room temperature. Afterwards, sodium chloroacetate was added, and this mixed solution was stirred in an oil bath at 55 °C with 6 h. After cooling to room temperature, a small amount of hydrochloric acid (0.1 M) was added into the simples and thus converting carboxyl groups to carboxyl acids. The CBC were obtained at last. The CBC was immersed in $NaIO_4$ solution (0.02 M) for 24 h. The obtained dialdehyde carboxymethyl bacterial cellulose (DCBC) was washed with deionized water for storage.

2.3. Preparation of the self-crosslinking dialdehyde carboxymethyl bacterial cellulose/chitosan composites (S-DCBC/CS)

The DCBC was immersed in CS solution for 24 h at room temperature. The CS solution can be obtained from 2 g CS dissolving in the 2% acetic acid solution. The obtained composites were repeated washed with deionized water and stored at 4 °C.

2.4. Determination of degree of aldehyde substitution

The aldehyde content of DCBC was subsequently quantified by Schiff base reaction with hydroxylamine. The preparation methods of hydroxylamine solution are same as the literature report [42]. HCl titrating solution (0.1 M) and NaOH standard solution (0.1 M) were obtained separately. NaOH standard solution was applied to titrate the HCl solution in the presence of phenolphthalein as the indicator solution. Adding acquired hydroxylamine solution (5 mL) and absolute alcohol (5 mL) into DCBC (0.1 g) sample and then the mixture was refluxed for 10 min. Then, HCl solution was used to titrate the mixture by watching the color change of the solution from yellow to green. The results were corrected by the blank tests. The degree of aldehyde substitution was calculated as follows:

$$degree\ of\ aldehyde\ substitution(\%) = \frac{162 \times N \times (V_1 - V_2)}{W} \times \frac{1}{2} \times 100 \qquad (1)$$

Where V_1 (L) is the volume of HCl solution consumed in DCBC samples, V_2 (L) is the volume of HCl solution consumed in blank samples, N (mol/L) is the normality of HCl solution, W (g) is the sample weight and the number 162 (g/mol) represents the relative molecular mass of one cellulose unit.

2.5. Characterization of S-DCBC/CS

FT-IR analysis was performed on a TENSOR II spectrometer (Bruker, Germany). The spectra were recorded with 16 scans and the resolution is 4 cm^{-1} at 4000-600 cm^{-1}. The samples were freeze-dried and then coated with a thin carbon film by sputtering. The microscopic morphology of the samples was observed with AURIGA Cross Beam FIB/SEM field emission electron microscopy; the acceleration voltage was 10 kV. To analyze the surface elements of samples, Energy Dispersive Spectroscopy (EDS) was tested in the same instrument.

To test crystalline state of the different samples, X-ray power diffraction (XRD) measurements were performed at 5 °C, on a Rigaku D/MAX-RB diffractometer (40 kV, 100 mA) with Cu Kα radiation, and the diffraction patterns were collected in the 2θ range from 10 to 90° at a scanning rate of 4°/min.

The surface roughness of BC, DCBC, CS and S-DCBC/CS were measured by atomic force microscopy (Dimension FastScan, Bruker, Germany) and Contour GT-K 3D Optical Profiler (Bruker, Germany). All of the samples need to be dried naturally to meet AFM testing requirements. All groups were measured in triplicate. The contact angles of BC, DCBC, CS and S-DCBC/CS were measured by contact angle measuring instrument (OCA15+, Dataphysics). The test liquids selected in the experiment was deionized water. Contact angle measurement was carried out in three different areas of the same sample.

Static tensile testing was conducted for BC, DCBC, CS and S-DCBC/CS in accordance with ASTM D 638-2003 Type IV specimens by TA-XT plus texture analyser at room temperature and humidity at a constant speed of 50 mm/min. The samples (n = 3) were tested in original hydrogel state.

2.6. Antibacterial activity test of different samples

The samples after sterilization were placed in 2 mL-centrifuge tubes including 100 μL diluted *E.coli* (or *S.aureus*)culture and 400 μL sterile liquid medium. The centrifuge tubes were placed in 37 °C temperature humidity chamber for 12 h. Then the samples were washed 2-3 times by PBS solution to remove the bacteria that do not adhere to the samples surface. The washed samples were placed in 500 μL medium and ultrasonic wave for 2 min in order to exfoliate adherent bacteria. 10 μL culture medium was taken out and evenly coated on the solid AGAR mediums. The solid AGAR mediums were taken photographs and counted the number of colonies after placing in the temperature humidity chamber for 24 h. The bacteriostatic rate was calculated by the following formula:

$$bacteriostatic\ rate(\%) = \frac{N_C - N_S}{N_C} \times 100 \quad (2)$$

Where N_C represents the colony count of control group and N_S represents the colony count of antibacterial samples.

The samples in 10 mm diameter were individually placed into a 24-well plate with one for per well, and the bacteria solution (3×10^4 CFU/mL, 500 μL) were inoculated into each well and cultured for 24 h at 37 °C. After the samples were rinsed thrice with 200 μL sterile PBS, each sample was stained with 600 μL of a dye solution that prepared from a mixture of SYTO fluorescent nucleic acid staining agents and propidum iodide in 5 mL deionized water for 15 min. Then the samples were observed *via* a fluorescence microscope (ZEISS Axio Vert. A1, Germany).

2.7. Cell culture, proliferation, migration and immunofluorescence staining

To investigate the migration of Human Umbilical Vein Endothelial Cells (HUVEC, Beijing Yuhengfeng Biotech Co. Ltd.) on samples, we used a microfluidic chip. The HUVEC was stained by Cell Tracker-green (Thermofisher Scientific, USA). The microfluidic chips were fixed on the surface of samples. Then 3×10^6 HUVEC suspension was injected into the microfluidic channel, then put into the incubator culturing for 4 h and peeled off microchip. The patterned cells on samples were observed by laser confocal microscopy at 0, 3, 6, 12 and 24 h. The reduction of the blank area is seen as the wound healing process.

To investigate the expression of Collagen-I, HUVEC were seeded on different samples and cultured 7 days. Then HUVEC were fixed by 3.7% formaldehyde, permeabilized with a rupture agent for 5 min, incubated with closed fluid for 1 h, primary antibody (Sigma-Aldrich, American) for 2 h at 37 °C. After that, the cells were incubated with rabbit polyclonal antibody (Sigma-Aldrich, American) for another 1 h. The nuclei were stained with Hochest 33342 (Dojindo, Japan), and observed with laser confocal microscopy.

2.8. Animal studies

Bama miniature pig weighing 7–8 kg were injected with Su-mian-xin II injection (0.15 mL/kg). The skin on the back was scalded for 30 s at 80 °C with the copper (d = 20 mm) of the digital temperature control scald apparatus. The specific experimental steps are as follows. Eight pigs, sex in half, were used in animal experiments. Deep II degree scald wounds were distributed in both sides of the spine in each pig. The infected wounds were made by inoculating 20 μL bacterial suspension (*Staphylococcus aureus* and *Pseudomonas aeruginosa*) to each wound. Then the wounds were covered with corresponding dressings separately (BC, CS and S-DCBC/CS). The CS dressings are the commercial dressing products (Guangzhou Keji Medical Instrument Co., LTD, Guangdong Device Registration Approval No. 20122640353) which have passed the CFDA certification. These animals were feed separately and normally without any other treatment. During the first 4 days, the frequency of dressing changing is once a day. The general observation was made at the different time points (0, 4, 8, 14, 20 and 28 days). Besides, some other operations, including sampling and bacteria counting, wound area measuring, photograph and binding wound up, are taken simultaneously. The situation of wound, including crusts formation, crusts falling off and anti-infection were recorded by visual inspection and photograph. In addition, the wound healing rate can be calculated as follows:

$$\omega\% = \frac{S_0 - S_n}{S_0} \times 100\% \quad (3)$$

The $\omega\%$ is the wound healing rate. S_0 and S_n are the wound area of the *0* day and the *n* day separately.

The samples for bacterial culture were collected from the wounds which were on the left and right side of pigs randomly. The time points are 4, 8, 14, 20 and 28 days after injury. This animal experiments were done by Beijing Dinghan Henghai Biotechnology Co., LTD and Beijing Dingguo Changsheng Biotechnology Co., LTD.

2.9. Histological and immunofluorescent staining

The wound tissues were taken for pathological examination. The wound tissue (width: 5–8 mm, depth: up to the sarcolemma) were sectioned along the spinal lateral. There was 5 mm normal skin at either end of wound tissue. All the tissues were fixed in 10% neutral formalin and embedded in paraffin. Hematoxylin and eosin (HE) immunohistochemical stain were performed and analyzed with microscopic examination. The observed contents included: epidermal growth, fibroblasts, new dermal collagen and the change of hair follicle and sebaceous glands close to the normal skin tissues. The HE staining slices were photographed by micrography.

After melting paraffin of tissue sections at 60 °C these sections were depafinized in xylene series. Placed in gradually decreasing ethanol series and distilled water for rehydration and then in hematoxylin solution for 10 min. Sections were dipped in distilled water after washing under tap water for few minutes. After 1% hydrochloric acid alcohol

differentiation, the sections were washed by current water for 10 min again. Placed in Ponceau's acid fuchsine solution for 5 min then dipped two times in distilled water and placed in phosphomolybdic acid solution for 5 min until the connective tissue becomes clear. Tissue sections were dipped into aniline blue solution for 5 min and into 1% glacial acetic acid for 1 min. Sections were dewatered by 95% ethanol and absolute alcohol in turn, and then were closed with neutral gum.

3. Results and discussion

3.1. Characterization of the S-DCBC/CS

Usually, chitosan/cellulose composites were prepared by means of solution casting that is a physical blending. Besides, an alternative approach is to add chemical crosslinking agent, including glutaraldehyde, borate, tripolyphosphate and so on. But we designed a bifunctional group modified BC which is both a matrix material and a crosslinker. The preparation method is shown in Fig. 1a. Some studies have shown that dialdehyde bacterial cellulose (DBC) can be obtained from BC by the $NaIO_4$-selective oxidation reaction. Chitosan can react with DBC by Schiff's base reaction (nucleophilic addition) in water, a crosslink composites can be prepared. The BC was firstly modified by carboxymethylation and the carboxyl groups (-COOH) was grafted onto BC. In fact, the carboxylic acid of the modified BC can enhance the electropositivity of amino because of the slightly acidic of carboxylic acid (Fig. 1b). In addition, the carboxyl can react with amino of CS and further enhance the crosslinking. The second effect of carboxyl group is hindering the bacteria absorbing trace elements and thus inhibits bacterial proliferation. In this study, the aldehyde group (-CHO) of dialdehyde carboxymethyl bacterial cellulose (DCBC) react efficiently with the amide group of CS, and the CS are fairly well distributed in the BC 3D network. The contacts between CS and fibers of BC are maintained by chemical bonds. In the process, toxic chemical crosslinking agent can be avoided.

As shown in Fig. 2, several ways were used to measure the physical and chemical properties of composites, including SEM, EDS, FTIR, XRD. Moreover, the mechanical properties and water holding capacity were also tested in this study. The results of SEM photos reveal that there's a total difference in BC's micro-sized morphology and structure before and after the modification. The fiber diameters of BC became thicker and a part of fibers were broken after carboxymethylated and selective oxidation modification. The carboxymethyl modification also increased the porosity of BC. Research shows that the change of the fiber diameter may be due to hydrogen bonds to break [43]. The fracture of fibers was the result of the selective oxidation by $NaIO_4$. The oxidation reaction results in the chemical bond rupture in the C2, C3 of the six-membered ring-like structure of D-glucose. The changes of fiber structure could have an impact on mechanical performance of DCBC. The microscopic structure of CS is significantly different from BC. The CS had no particular distinguishing features in morphology on the condition of high magnification but had three-dimensional porous structure at lower magnifications (Fig. S1). The structural characteristics could be related to the treatment method that is freeze-drying after dissolve. The microstructure of S-DCBC/CS that the fibers are linked together by chitosan crosslinking reaction is remarkably different from that of other samples. The crosslinking and chitosan penetration didn't change the fiber diameter of DCBC. But the hole size of composites became large after the self-crosslinking. The large size of hole will help to absorb tissue exudate. The micro-pore structure of CS scale to nano-pore structure due to the composite between CS and BC. This nanoscale

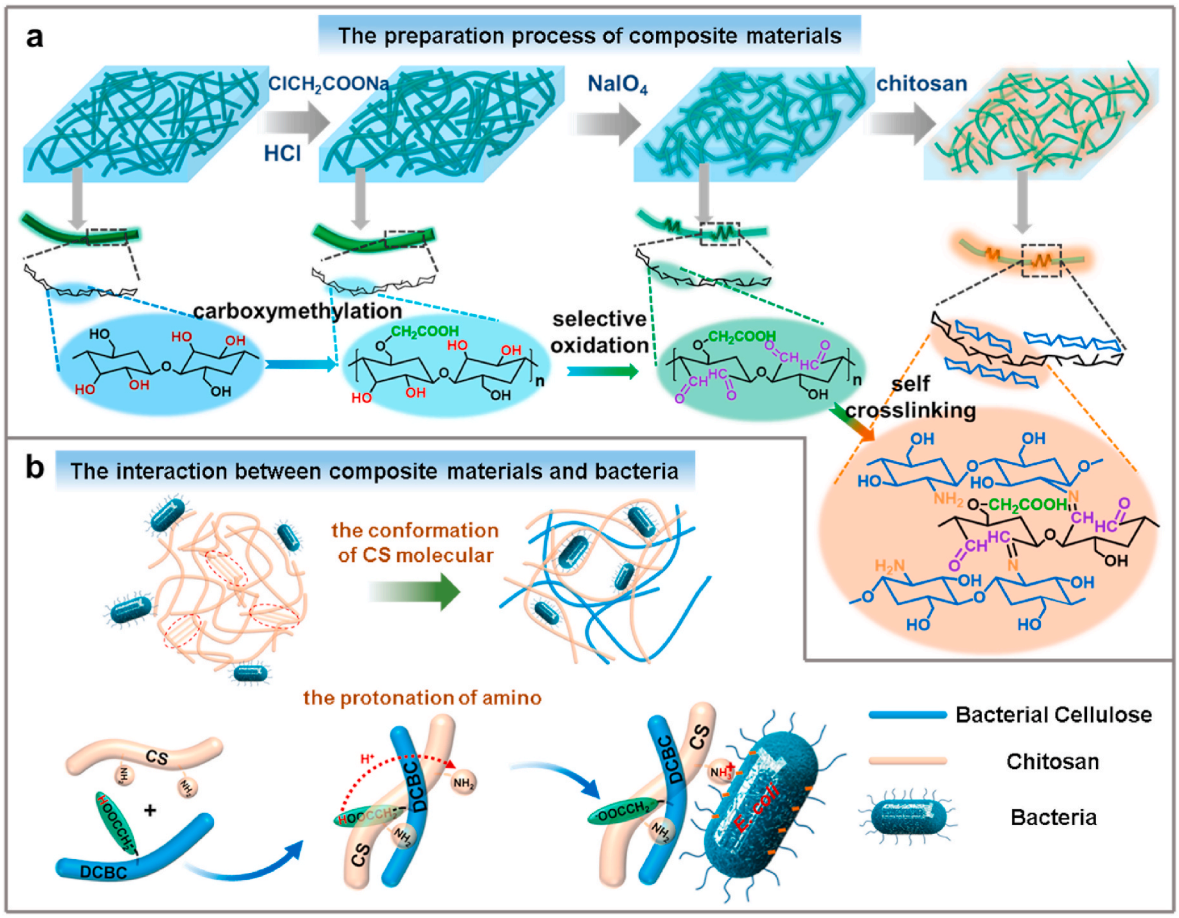

Fig. 1. Schematic diagram of the preparation of S-DCBC/CS by self-crosslinking reaction and antimicrobial effects of composites (*E. coli*).

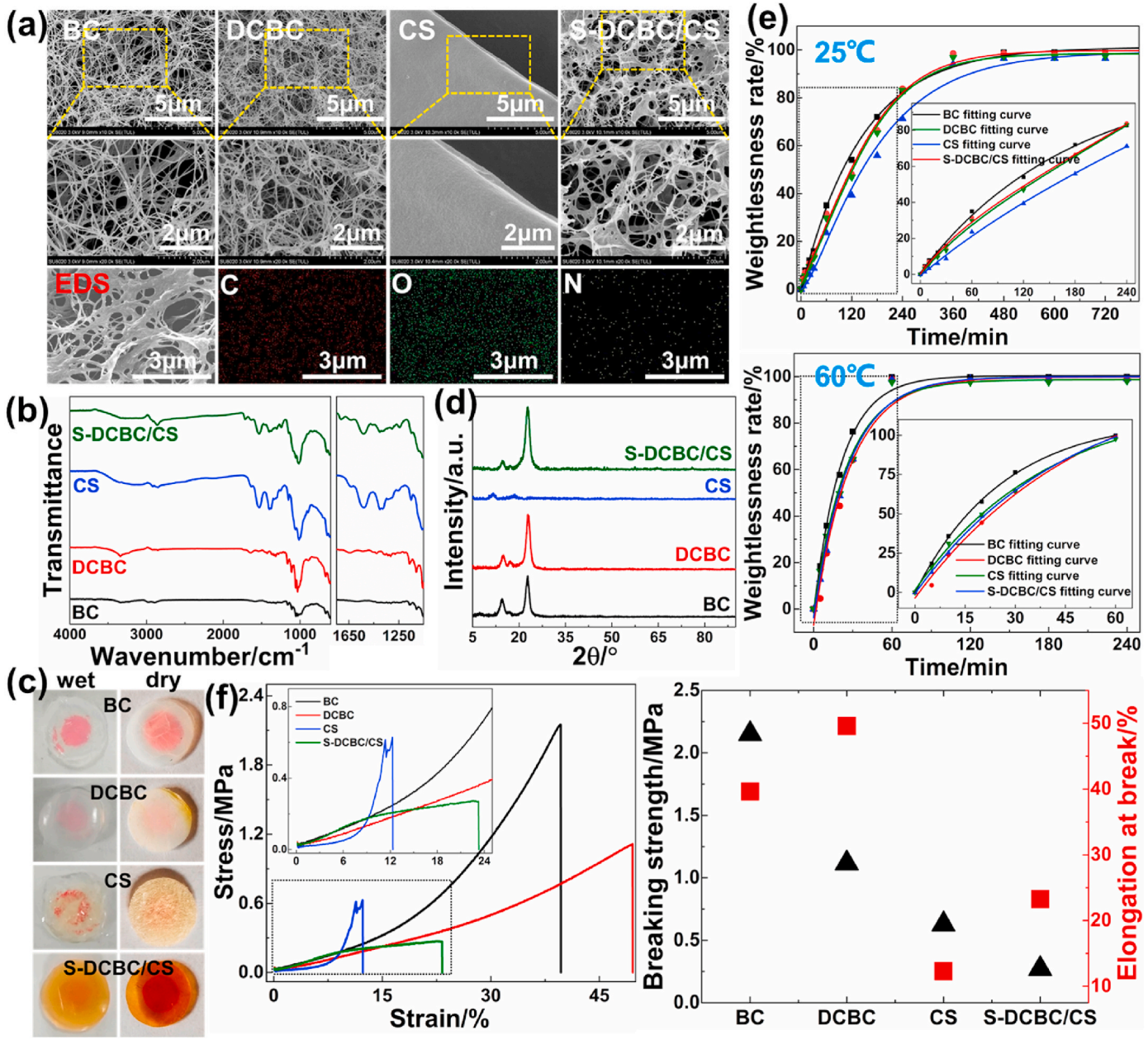

Fig. 2. (a)SEM and EDS, (b) FTIR, (c) Transparency contrast under wet and dry states, (d) XRD, (e) The water holding capacity (25 °C and 60 °C), (f) Mechanical properties of BC, DBC, CS and S-DBC/CS.

structures are conducive to the functional groups (mainly amino of CS) exposed clearly and these functional groups could improve the antibacterial activity and biocompatibility.

The FT-IR spectrum of different samples are shown in Fig. 2b. The spectra of the sample of BC have shown strong signals at 3350, 2910, and 1050 cm^{-1}. These signals correspond to the characteristic absorption peak of BC. After carboxymethylation, the carboxyl group (-COOH) was grafted on the molecular of BC. The FT-IR spectrum of carboxymethyl bacterial cellulose (CBC) is different from the BC's (Fig. S2). These peaks including 1560 cm^{-1}, 1410 cm^{-1} came from the antisymmetric and symmetric stretching vibrations of -COOH. For DCBC, the peak at 1650 cm^{-1} was the carbonyl absorption band that came from the selective oxidation. The FTIR spectra helped to verify the success of carboxymethylation and selective oxidation modification. For the FTIR spectrum of CS, a broad peak existing between 3500 and 3100 cm^{-1} corresponds to the stretching vibrations of N-H and O-H [44]. Two peaks at 1650 and 1560 cm^{-1} are attributed to the C=O in the amide group and N-H bending vibration of the amine group, respectively [45]. The bands between 1100 and 1000 cm^{-1} are assigned to C-N and C-O stretching vibrations. The absorption at 1700 cm^{-1} and 1570 cm^{-1} resulted from C=N bond and C-N bond verifying the formation of the Schiff's base occurred between the oxidized cellulose and chitosan. The absorption peaks of DCBC and CS spectra were reflected in the S-DCBC/CS spectrum [46].

The X-ray diffractograms of BC, DCBC, CS and S-DCBC/CS are also presented in Fig. 2d. In the XRD spectrum of BC, three peaks can be observed. These peaks are typical for cellulose, the Bragg angles are respectively 14.57°, 16.97°and 22.81° corresponding to (110), ($1\bar{1}0$) and (200) crystal planes of cellulose. The three peaks are characteristic peaks of cellulose I crystals. This is consistent with the literature report [47]. The characteristic peaks of cellulose also can be observed in the XRD spectrum of modified BC and composites, and there are no characteristic peaks of CS ($2\theta = 10°, 20°$) in the spectrum of composites. It can be explained that the CS molecule was amorphous in the composites.

This amorphous distribution of CS molecule exposes more amino groups and increases the contact area between CS molecule and bacteria (Fig. 1b). These characteristics will contribute to the improvement of antibacterial activity of S-DCBC/CS.

A moist environment can promote the penetration of the active substances, protect wounds against bacterial invasion, and provide a painless removal from wound surface after recovery [48]. An ideal wound dressing should lock the exudate, as well as maintain proper wound moisture during the healing process. Therefore, the water retention capacity of the S-DCBC/CS dressings were measured at 25 °C and 60 °C. These data are presented in Fig. 2e. The water retention of DCBC and S-DCBC/CS is no significant difference. The water retention of S-DCBC/CS is better than that of pure BC and second only to CS. Besides, the water retention of S-DCBC/CS is still better than that of pure BC and closer to that of CS at 60 °C. Compared with other samples, the water retention characteristic of S-DCBC/CS composites stand out more under 60 °C. Thus, from a moisturizing perspective, the S-DCBC/CS composites which is similar to the BC could be used for wound dressing. It was worth noting that the transmittance of composites is better than that of dried CS. This is due to the amorphous state of CS molecular structure. From the BC point of view, chitosan addition or crosslinking reduced the light transmission of BC (Fig. 2c). But the composites still retain a fair amount of transmittance which can help to observe the wound healing and exudation condition when it is used as a dressing. For the mechanical property, breaking strength of the composites was decreased after modification. This is related to the aldehyde modification of BC. The degree of aldehyde substitution of DCBC is 22.13%. To a certain extent, this degree of aldehyde substitution could maintain the mechanical property of DCBC and provide sufficient aldehyde. But the hydrogen bonding and covalent bonding of BC were still broken during the modification. The dressing needs to have good flexible and adhesion rather than too high strength, just like the gel dressing, so the breaking

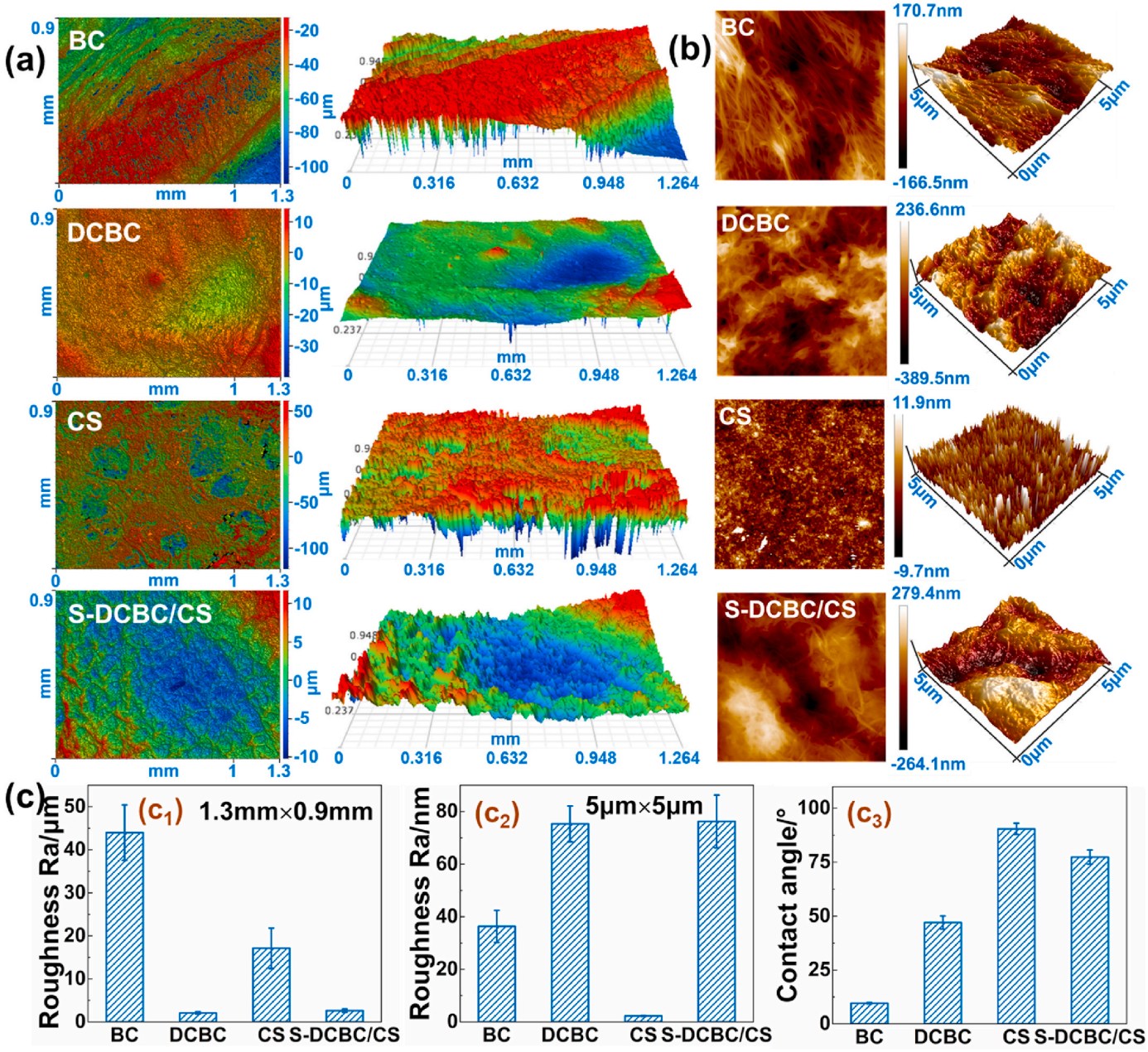

Fig. 3. Surface performance (a) Surface 3D morphology at the millimeter scale by 3D Optical Profiler (b) Surface 3D morphology at the micron scale by AFM (c) the data of Roughness and Contact Angle.

strength and elongation at break of S-DCBC/BC reached 25 KPa and 23% respectively which still could meet the requirements of wound dressing. In addition (Fig. S3), it was noticeable that the CS showed tear layer upon layer.

3.2. Surface performance analysis

In the field of biomaterials, the surface performance of composites is important to the cell proliferation and adhesion. Hence, the surface roughness, surface topography and hydrophilicity were tested by AFM, 3D Optical Profiler and contact angle meter. The testing results of surface properties were shown in Fig. 3. As shown in Fig. 3a and c_1, the surface roughness of BC was greater than other samples at the millimeter scale. This is ascribable to the fact that there are many folds on the BC surface after dried at room temperature. The roughness of CS was also bigger than DCBC and S-DCBC/CS which was due to the three-dimensional porous structure of CS which came from the freeze-drying of CS solution.

AFM is one of the tools to study surface roughness as a function of layers because its ability to scan surface morphology at small scales. Therefore, as shown in Fig. 3b, the surface topography of composites was measured by AFM at the micron scale. Compared with the roughness at millimeter scale, the roughness of BC and CS was less than the other samples at micron scale. Fig. 3b shows the surface topography of different samples. It is possible to see that the morphology changes of BC after modification. Pure BC has obvious nanofiber structure, but the fiber morphology of DCBC was not obvious. This was due to the breaking hydrogen bonds and fracture of chemical bonds which led to the crystal structure of BC be broken. The fiber morphology of S-DCBC/CS was more ambiguous than DCBC, because the CS molecule was filled in the 3D network of BC fibers. For the hydrophilicity and contact angle, the images of contact angle were shown in Fig. S4 and the statistics was shown in Fig. 3c_3. The contact angle of CS and S-DCBC/CS was bigger than pure BC and modified BC. The contact angle of BC was lower than 10°. However, studies have shown that the BC surface was too smooth to benefit cell adhesion and growth. The S-DCBC/CS surface with certain roughness was more favourable for cell growth.

3.3. The antimicrobial properties

E. coli and *S. aureus* incubated with BC, DCBC, CS and S-DCBC/CS were dyed with a LIVE/DEAD fluorescence kit to analyze the antibacterial activity of different samples. Under fluorescence microscope, viable bacteria appear as green and dead bacteria appear as red color. The fluorescent micrographs revealed that most of the bacteria (*E. coli* and *S. aureus*) were alive well on the surface of BC and DCBC. BC and

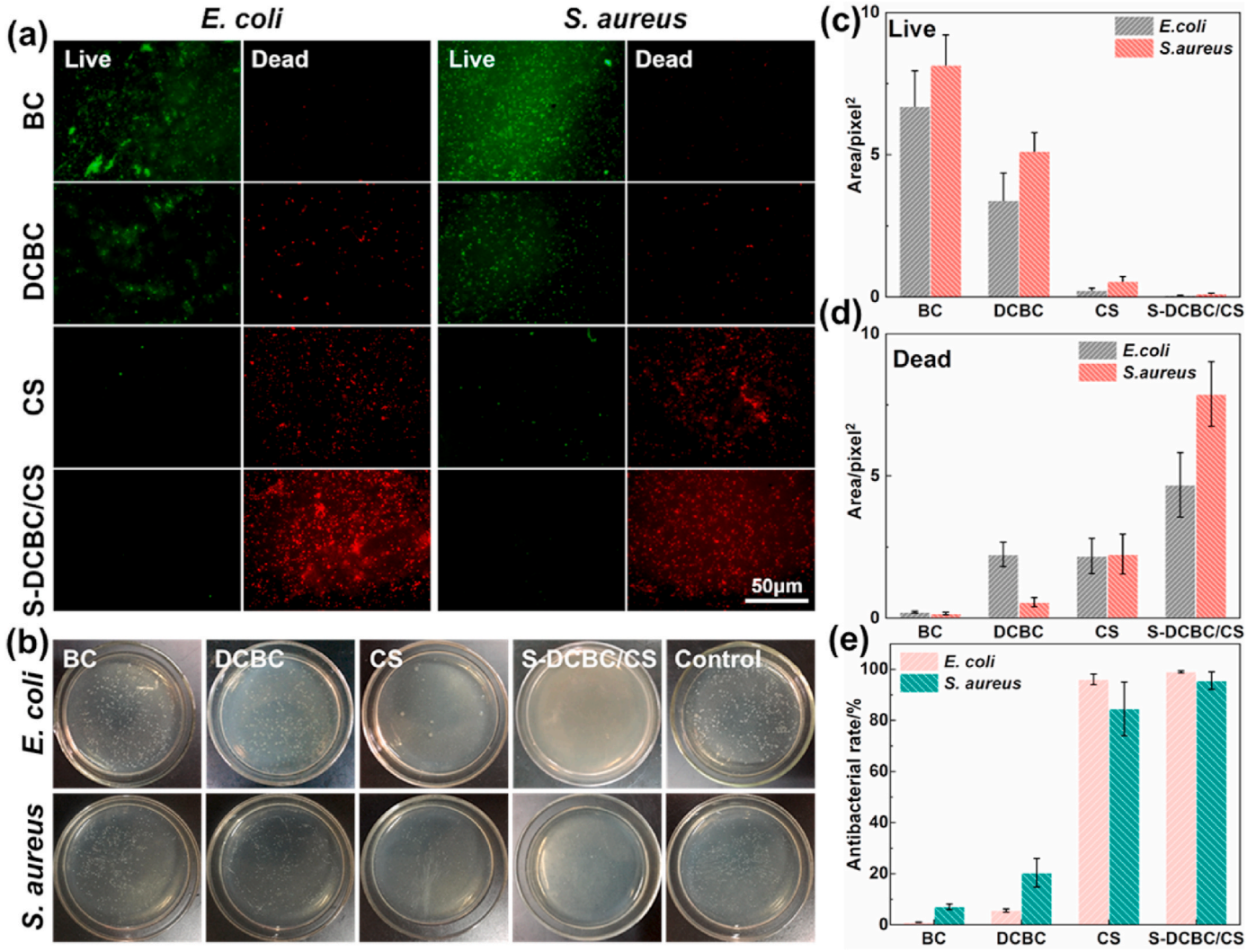

Fig. 4. (a) Fluorescence micrographs of *E.coli* and *S.aureus* incubated on the surfaces of BC, DCBC, CS and S-DCBC/CS. (b) The plate colony-counting experiments of BC, DCBC, CS and S-DCBC/CS. (c) Statistics of the area live of bacteria on surfaces with different samples. (d) Statistics of the area of dead bacteria on surfaces with different samples. (e) Inhibition rate of the different samples.

DCBC don't show antibacterial activity. The results of CS and S-DCBC/CS was contrary to BC and DCBC. The live bacteria (*E. coli* and *S. aureus*) almost don't exist on the surface of CS and S-DCBC/CS. The CS and S-DCBC/CS show excellent antibacterial activity against *E. coli* and *S. aureus*. As shown in Fig. 4b, in order to investigate the antibacterial activity further, the colony-count method was used to test the bacteriostatic rate of different samples. The results showed that the bacteriostatic rates of BC and DCBC were generally lower than 10%. However, the bacteriostatic rates of CS and S-DCBC/CS higher than 90%, even more 99%. The CS and S-DCBC/CS show excellent antibacterial activity. The results of colony count experiment displayed a satisfied consistence with live/dead dyeing experiments.

In particular, as we can see from Fig. 4e, the inhibition rate of S-DCBC/CS was a little higher than CS. Some researches [49,50] show that the carboxyl group could promote chitosan to adsorb trace elements. These elements are extremely important for bacterial proliferation. Besides, the carboxyl group can improve the electropositivity of amino of CS, to a certain extent. Thus, the carboxyl group of BC could enhance antimicrobial activity of CS. More importantly, the molecule structure of chitosan become amorphous in the 3D network of BC, which would expose more amino groups and increase contact area with bacteria. Amino is the most important group to the antibacterial activity of CS. In addition, there is another important point to be noted. The fluorescent dye images and bacteria area statistics show that the total bacterial count of S-DCBC/CS higher than that of CS. This phenomenon has to do with the 3D nano-network structure and high moisture of composites. The nano-network structure is good for bacterial adhesion and the high moisture characteristics favor the survival of bacterial. In other words, relative to CS, bacteria tend to stick on the surface of S-DCBC/CS. The S-DCBC/CS could promote bacteria adhesion, then to kill them. This characteristic is called "active" antibacterial action in this study.

3.4. Cell compatibility and migration

The cell biocompatibility of different samples was studied by several methods. Mouse fibroblast (L929 cells) was often used to test the biocompatibility of materials. Therefore, the L929 cells were cultured on different samples surface for 3 days and were observed with fluorescence microscope. As shown in Fig. S5, the cell number of CS and S-DCBC/CS were significantly greater than DCBC. Besides, the cytocompatibility of pure BC was also better than DCBC. This is related to the large of aldehyde group which come from the selective oxidation modification. The aldehyde group is disadvantage to the cell proliferation and adhesion. After self-crosslinking reaction, the cytocompatibility of composites was significantly better than pure BC. This is because that the aldehyde groups of DCBC are consumed by self-crosslinking reaction and the CS has better biocompatibility than pure BC.

Collagen-I synthesized by endothelia cell is a kind of structural protein in animal skin. The metabolism of collagen-I directly affects the repair quality of the wound. Therefore, the HUVEC also was seeded on different samples surface and the collagen-I was observed by fluorescence microscope after Immunofluorescence staining. From the immunofluorescence staining images of Fig. 5a, it can be seen that S-DCBC/CS can significantly promote the expression of collagen-I in HUVEC. The number of nuclei on S-DCBC/CS is more than pure BC and DCBC, indicating that S-DCBC/CS can promote the proliferation of HUVEC. The number of nuclei and expression of collagen-I on DCBC are the least. This is also due to the large amount of aldehyde groups in the BC fiber. The excellent biocompatibility and high Collagen-I expression of S-DCBC/CS benefited from the biocompatibility of CS and the Schiff's base reaction between aldehyde group of DCBC and amino of CS.

To study the effect of composites on the cell migration, we implemented a microfluidic device that allows quantitatively evaluating the collective cell migration on materials. As shown in Fig. 5b, different from the scraping line method, our device employed a special configuration to facilitate quantitative measurement for cell migration [51]. The cell migration process can be dynamically depicted by quantifying the blank area among cells where was previously occupied by exclusive post in the microfluidic chip. As can be seen from Fig. 5c, the HUVEC migration were characterized by the laser confocal microscope at different time point of 0 h, 3 h, 6 h, 12 h and 24 h. The results showed that compared with other materials, the HUVEC present the fastest migration on the CS and S-DCBC/CS. The HUVEC almost recovered the blank space of S-DCBC/CS in 6 h. The migration rate of CS is close to the composites. But the cell migration of S-DCBC/CS is higher than the other samples in 3 h. The HUVEC recovered the "wound" more rapidly on S-DCBC/CS whereas the S-DCBC exhibit the poorest biocompatibility for supporting cell migration even compared with BC (Fig. 5c and d). The results indicated that the good biocompatibility of S-DCBC/CS benefited from the grafting of CS which could consume the aldehyde group of the DCBC. The empty area data of BC, CS and S-DCBC/CS were not quite different. But the migration rate of S-DCBC/CS was higher than the other samples obviously before 9 h. Moreover, the migration speeds of HUVEC which is obtained from the slope of the migration rate curve on S-DCBC/CS was also faster than other samples. This also showed that the S-DCBC/CS had good influence on the HUVEC proliferation and migration and would be conducive to wound healing.

3.5. In vivo infeviacted wound healing of S-DCBC/CS

Wound situation was evaluated for each group on days 4th, 8th, 14th, 28th and healing situation images were represented on Fig. 6. Wound area was photographed and wound area (mm^2) was calculated using a computer software (Image J) (Fig. 6d). The rest of healing images were listed on Supplementary information (Fig. S6). Data obtained from these calculations were evaluated using statistical methods. The wound was porcelain white after deep II degree scald and had mild swelling. Then the skin of wounds region started to change color and formed crusts. The color of skins changed, in turn, from porcelain white to pink, brown or light brown then, and black last. The skin also changed from soft to hard. On the 4th day, scald area showed an obvious dividing line with normal tissue. The wound manifested as tissue hyperemia, local brown and a red border that tended to wear off after 14 days. On the 8th day after injury, all of the wounds formed crusts and some crusts began to come off naturally. Most of the crusts sloughed off obviously and a few of new epithelium started to form 14 days after injury. The wound closed up 28 days later.

According to the wound healing statistics (Fig. 6d), wound healing rate in each group was about 10% 4 days after injury. The wound healing rate of group S-DCBC/CS increased by more than 50% after 14 days, significantly higher than that of group BC. The healing rate of S-DCBC/CS and CS was even higher as 80% after 28 days. From the entire healing process, the healing rate of S-DCBC/CS was evidently higher than that of group BC and CS. This result indicated that the S-DCBC/CS has an effect in promoting burn wound healing.

Moreover, bacterial cultures were made on these wounds that were selected randomly. This result was shown in Fig. 6c and the statistical results of colony count was found in Table S1. The colony count of all the groups was gradually reduced with time growing after injury. The wounds treated with S-DCBC/CS and CS had significantly less colony than the group BC ($P < 0.01$). It has been proved that CS is a basic polysaccharide in the nature that has good antibacterial ability. DCBC can be modified by CS to improve the micro-organism resistance. But the amino of CS is consumed by self-crosslinking reaction. There will be a potentially decrease in antimicrobial performance. But the results of animal experiments rarely showed the decrease of antibacterial activity. Instead of decreasing, as shown in Fig. 6c, the antibacterial activity of group S-DCBC/CS was a litter better than CS group. This result were consistent with the bacteria live/dead dyeing. We believed that was mainly benefited from the carboxymethylated modification of BC. Previous research has shown that the carboxylic group can improve the antibacterial activity of CS.

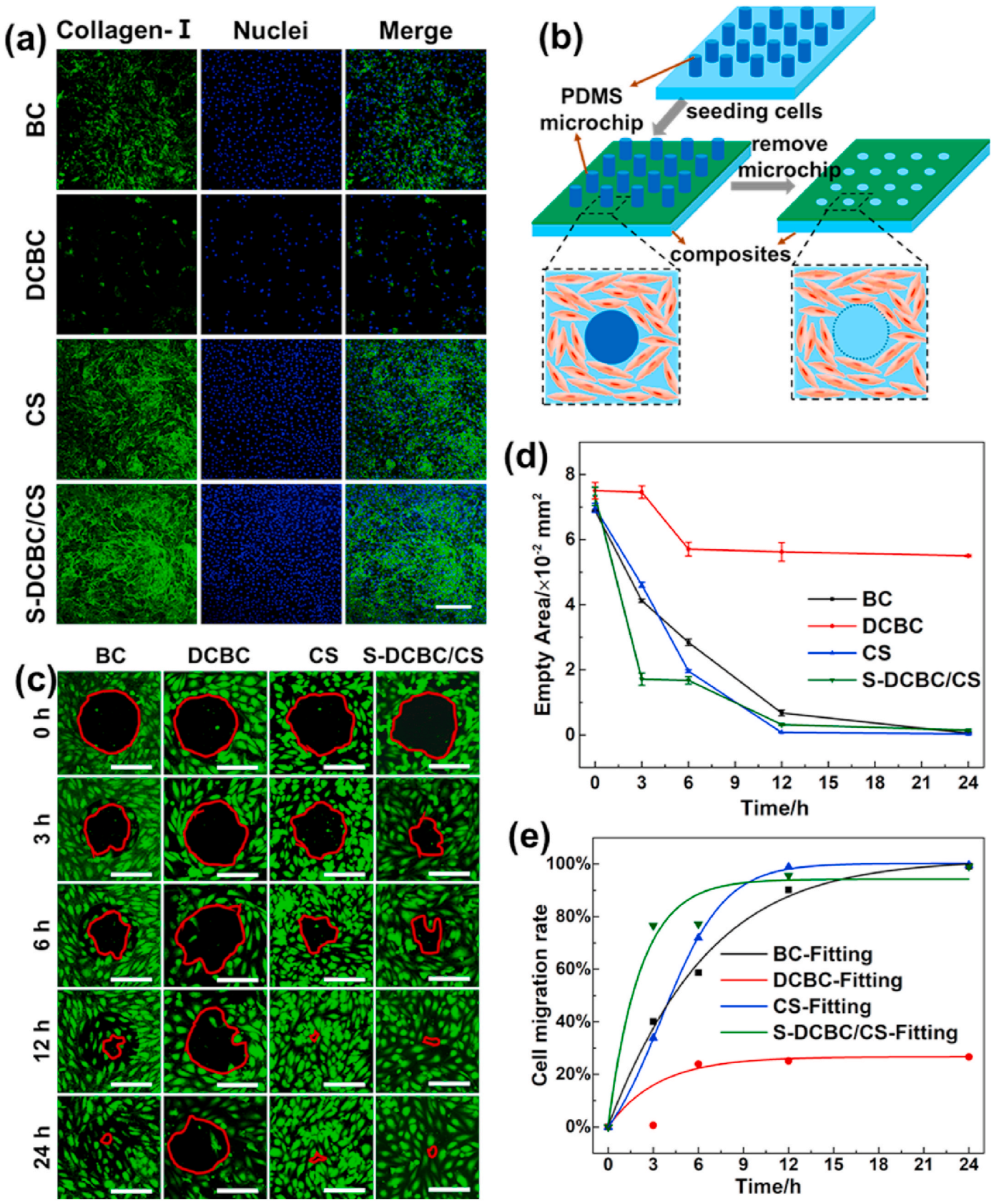

Fig. 5. (a) Morphology of HUVEC stained against Collagen-I (green) and Hochest stained nuclei (blue) at day 7 on different samples (The scale bar is 300 μm), (b) The schematic diagram of studying cell migration by microfluidic chip, (c) Migration of HUVEC pictured by Confocal Microscope on BC, DCBC, CS and S-DCBC/CS (The scale bar is 300 μm), (d) (e) The normalized empty area and migration rate of HUVEC on BC, DCBC, CS and S-DCBC/CS.

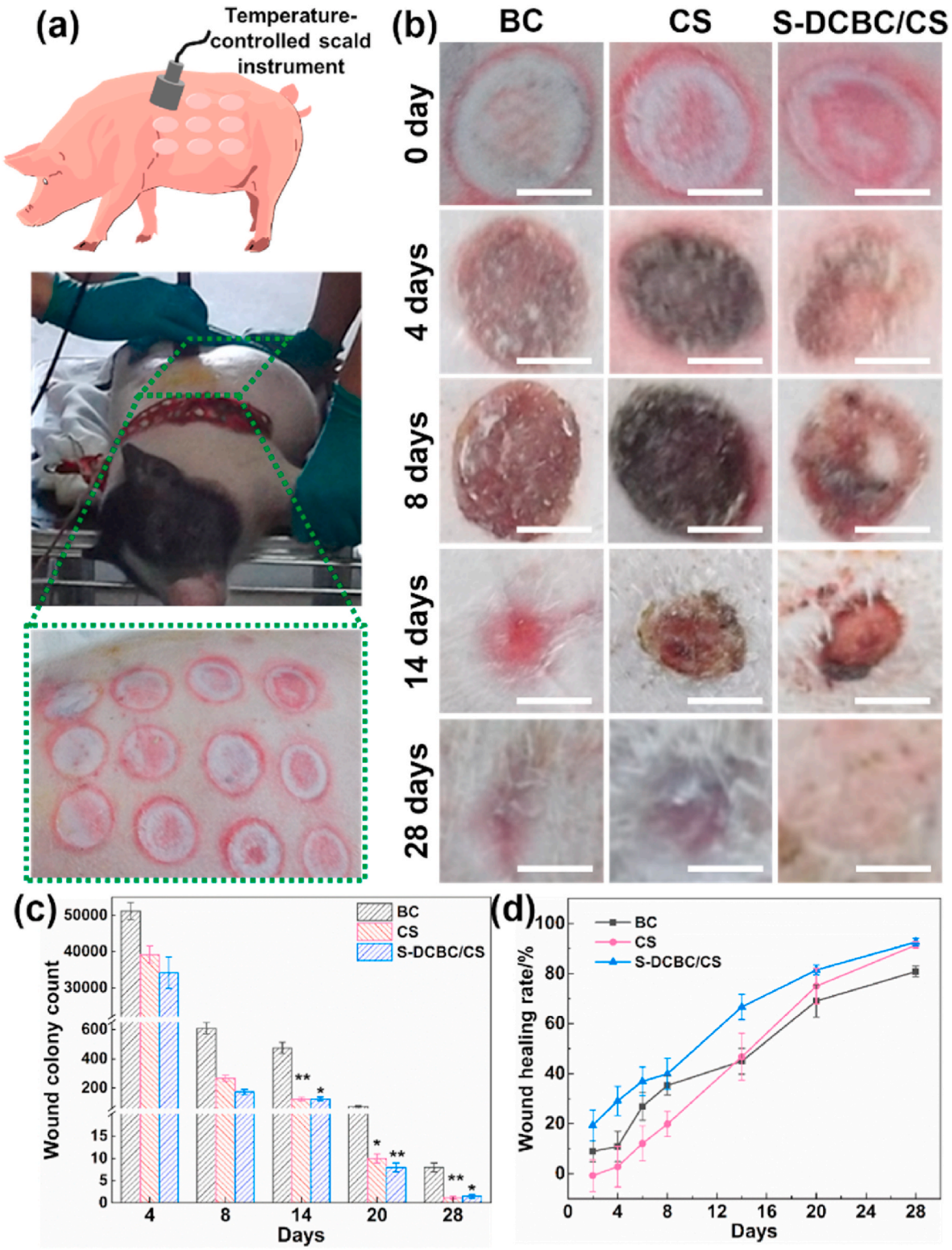

Fig. 6. (a) The photographs show the deep second-degree scald wounds on the back of the Bama miniature pig (The scale bar is 10 mm), (b) Schematic showing the building of deep II degree scald wounds pig model by Temperature-controlled Scald Instrument. The wound colony count (c) and the wound healing rate (d) after treatment with the different materials (BC, CS and S-DCBC/CS) at different time points (days). (Compared with the BC, *P < 0.01, **P < 0.001).

To further investigate the wound healing progress, histological determination including H&E and Masson's trichrome staining were performed as shown in Fig. 7. Microscopic images obtained from the tissue sections' histochemical staining (Hematoxylin Eosin and Masson's Trichrome staining) are presented in Fig. 7a and b. From the HE staining of 4 days, the coagulative necrosis of epidermal layer and papillary layer can be observed under the microscope. The subdermal vascular network close to necrotic tissue were hyperemia. Especially in Group BC, the epidermis and dermis were necrotic and showed tissue fusion between epidermis and dermis, unclear composition and severe damage. All of

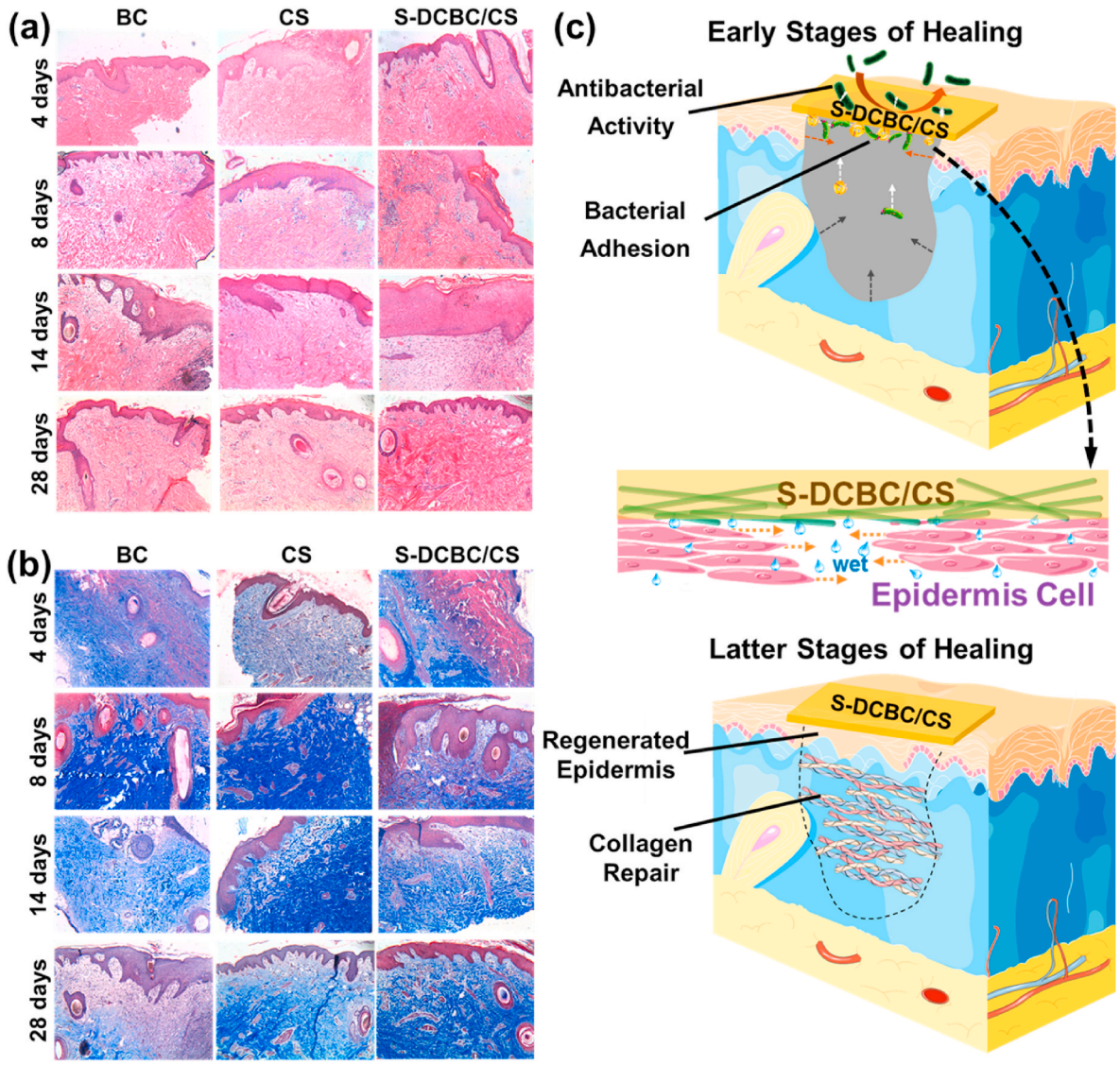

Fig. 7. H&E (100 ×) stained section(a) and Masson's trichrome (100 ×) stained section (b) of regenerated wound tissue treated with the different materials (BC, CS and S-DCBC/CS) at different time points (days). (c) Schematic illustrations of wound healing process by using S-DCBC/CS.

the groups were covered with scab in 8 days after injury and the new skin tissues could be seen under the scab by the microscope. After 14 days, it has been observed for these samples that most of the wounds healed well and the collagen in the dermis was tight. In contrast, the reparative effect of group CS and S-DCBC/CS was better than BC group. At the four weeks after injury, the wounds were entirely covered with new skin which the structure was mature. It was seen for the tissue biopsies that collagenous fibers of deep dermis were arranged more orderly. The new capillaries and fibroblasts could be observed under the dermis. Epithelial island was from focal nodular hyperplasia to regional hyperplasia and hair follicle proliferated actively. The group of S-DCBC/CS and CS had a better recovery than the group of BC obviously. The result of tissue biopsies also showed that the S-DCBC/CS had the performance of promoting wound healing.

The result of Masson's Trichrome staining is shown in Fig. 7b. Main layers of the skin such as epidermis, dermis and hypodermis, reticular and papillary sub layers of dermis and skin adjuncts such as hair follicles and wens were evident by both staining studies. The trichrome stain highlights the collagen fiber in blue. The epidermis, the blood vessels of dermis, lymphatic vessels, hair follicles, sebaceous glands, sweat glands, muscle fibers and fibroblasts were stained red and the nuclear stained in blue-black. As Fig. 7 shows, coagulation necrosis area of the upper dermis was reddish in the tissue slides. The changes of skins in the Masson's Trichrome staining were similar to the corresponding HE staining slice.

Given the above, compared to BC, the S-DCBC/CS can promote wound healing and prevent bacterial contamination. As shown in Fig. 7c, in the early stages of wound healing, the primary role of S-DCBC/CS dressing is boosting the wound's ability to retain moisture as well as to keep germs from seeping into the body. The humid conditions and special nanostructure of S-DCBC/CS dressing can promote epidermal cells multiplication. The bacteria tend to directional move and adhere to the surface of S-DCBC/CS dressing, and then be killed by the antibacterial ingredients. Moreover, the S-DCBC/CS dressing also helps the dermal collagen repair during the wound-healing process. These conclusions are supported by dead/alive staining results of bacteria and histological observation. It's worth noting that no significant differences were observed in epidermis growth between S-DCBC/CS and CS. However, the promoting concrescence of S-DCBC/CS is obvious better than CS. It could be due to the positive impact of BC on collagen tissue repair because of the wet healing. So, the S-DCBC/CS has the best promoting healing effect in our study. The promoting healing ability and antibacterial activity of composites reach to those of commercial dressing. The S-DCBC/CS could be used as a wound dressing.

4. Conclusions

In summary, a kind of novel bifunctional group modified BC was prepared by carboxymethylation and selective oxidation. Then, a functional S-DCBC/CS composites with the DCBC as the base material and crosslinking ingredient was also prepared further. The S-DCBC/CS composites could promote cell proliferation and migration, and then lead to the wound healing. The XRD shows that the crosslinking and chitosan penetration have little effect on the crystallinity of modified BC. S-DCBC/CS composites have a better water retention than pure BC and could provide moist environment. The bacteriostatic rate of composites can reach 99% because of the amorphous distribution of CS molecules in the composites and the influence of carboxyl groups. The S-DCBC/CS with a good effect on bacteria adherence could attract bacteria adhesion and kill them. The cell migration of S-DCBC/CS is the highest in 3 h. Thus, composites have a good influence on the HUVEC proliferation and migration. In the deep II degree scald wounds healing of large animal model, the S-DCBC/CS composites could promote epidermal growth and collagen production in two weeks. The promoting healing ability and antibacterial activity of S-DCBC/CS composites are same as the commercial dressing, or even better.

CRediT authorship contribution statement

Yajie Xie: Conceptualization, Investigation, Writing – original draft. **Kun Qiao:** Visualization, Data curation. **Lina Yue:** Investigation, Validation, Writing – review & editing. **Tao Tang:** Resources, Investigation. **Yudong Zheng:** Supervision, Funding acquisition, Writing – review & editing. **Shihui Zhu:** Supervision, Writing – review & editing. **Huiyi Yang:** Investigation. **Ziyuan Fang:** Investigation.

Declaration of competing interest

The authors declare that they have no known competing financial interests or personal relationships that could have appeared to influence the work reported in this paper.

Acknowledgements

This work was financially supported by National Natural Science Foundation of China (Grant No .51973018, 51773018); Beijing Municipal Science and Technology Commission Projects (No. Z191100002019017); Key Research and Development Projects of People's Liberation Army (BWS17J036); National Key Research and Development Project (No.2019yfa0110603), Program for the Top Young Talents of Higher Learning Institutions of Hebei (BJ2021096), The fellowship of China Postdoctoral Science Foundation (No.2020T130005ZX).

Appendix A. Supplementary data

Supplementary data to this article can be found online at https://doi.org/10.1016/j.bioactmat.2022.01.018.

References

[1] R. Poonguzhali, S.K. Basha, V.S. Kumari, Novel asymmetric chitosan/PVP/nanocellulose wound dressing: in vitro and in vivo evaluation 112 (2018) 1300–1309.
[2] T. Maver, S. Hribernik, T. Mohan, D.M. Smrke, U. Maver, K.J.R.A. Stana-Kleinschek, Functional wound dressing materials with highly tunable drug release properties 5 (95) (2015) 77873–77884.
[3] J. Wu, C. Su, L. Jiang, S. Ye, X. Liu, W.J.A.S.C. Shao, Engineering, Green and facile preparation of chitosan sponges as potential wound dressings 6 (7) (2018) 9145–9152.
[4] Z. Hadisi, J. Nourmohammadi, S.M.J.I. Nassiri, The antibacterial and anti-inflammatory investigation of Lawsonia Inermis-gelatin-starch nano-fibrous dressing in burn wound 107 (2018) 2008–2019.
[5] M.C. García, A.A. Aldana, L.I. Tártara, F. Alovero, M.C. Strumia, R.H. Manzo, M. Martinelli, A.F.J.C.p. Jimenez-Kairuz, Bioadhesive and biocompatible films as wound dressing materials based on a novel dendronized chitosan loaded with ciprofloxacin 175 (2017) 75–86.
[6] M.W. Ullah, M. Ul-Islam, S. Khan, Y. Kim, J.K. Park, Innovative production of bio-cellulose using a cell-free system derived from a single cell line, Carbohydr. Polym. 132 (2015) 286–294.
[7] S. Ifuku, M. Nogi, K. Abe, K. Handa, F. Nakatsubo, H.J.B. Yano, Surface modification of bacterial cellulose nanofibers for property enhancement of optically transparent composites: dependence on acetyl-group DS 8 (6) (2007) 1973–1978.
[8] M. Nogi, H.J.A.M. Yano, Transparent nanocomposites based on cellulose produced by bacteria offer potential innovation in the electronics device industry 20 (10) (2008) 1849–1852.
[9] D. Lin, Z. Liu, R. Shen, S. Chen, X. Yang, Bacterial cellulose in food industry: current research and future prospects, Int. J. Biol. Macromol. 158 (2020) 1007–1019.
[10] C.K. Chan, J. Shin, S.X.K. Jiang, Development of tailor-shaped bacterial cellulose textile cultivation techniques for zero-waste design, Cloth. Text. Res. J. 36 (1) (2018) 33–44.
[11] J. Caro-Astorga, K.T. Walker, N. Herrera, K.-Y. Lee, T. Ellis, Bacterial cellulose spheroids as building blocks for 3D and patterned living materials and for regeneration, Nat. Commun. 12 (1) (2021) 1–9.
[12] D.A. Gregory, L. Tripathi, A.T. Fricker, E. Asare, I. Orlando, V. Raghavendran, I. Roy, Bacterial cellulose: a smart biomaterial with diverse applications, Mater. Sci. Eng. R Rep. 145 (2021) 100623.
[13] S.C. Fernandes, L. Oliveira, C.S. Freire, A.J. Silvestre, C.P. Neto, A. Gandini, J.J.G. C. Desbriéres, Novel transparent nanocomposite films based on chitosan and bacterial cellulose 11 (12) (2009) 2023–2029.
[14] N. Lin, A.J.E.P.J. Dufresne, Nanocellulose in biomedicine: current status and future prospect 59 (2014) 302–325.
[15] H. Zahedmanesh, J.N. Mackle, A. Sellborn, K. Drotz, C.J.J.B.M.R.B.A.B. Lally, Bacterial cellulose as a potential vascular graft: mechanical characterization and constitutive model development 97B (1) (2015) 105–113.
[16] N.H. Silva, A.F. Rodrigues, I.F. Almeida, P.C. Costa, C. Rosado, C.P. Neto, A. J. Silvestre, C.S.J.C.p. Freire, Bacterial cellulose membranes as transdermal delivery systems for diclofenac: in vitro dissolution and permeation, Studies 106 (2014) 264–269.
[17] A. Müller, Z. Ni, N. Hessler, F. Wesarg, F. Müller, D. Kralisch, D.F.J.J.o.P. Sciences, The biopolymer bacterial nanocellulose as drug delivery system: investigation of drug loading and release using the model protein albumin 102 (2) (2013) 579–592.
[18] L. Fu, J. Zhang, G.J.C.p. Yang, Present status and applications of bacterial cellulose-based materials for skin tissue repair 92 (2) (2013) 1432–1442.
[19] M. Rouabhia, J.r.m. Asselin, N. Tazi, Y.s. Messaddeq, D. Levinson, Z.J.A.a. m. Zhang, interfaces, Production of biocompatible and antimicrobial bacterial cellulose polymers functionalized by RGDC grafting groups and gentamicin 6 (3) (2014) 1439–1446.
[20] N. Lin, A.J.E.P.J. Dufresne, Nanocellulose in biomedicine: current status and future prospect 59 (2014) 302–325.
[21] J. Wu, Y. Zheng, X. Wen, Q. Lin, X. Chen, Z.J.B.m. Wu, Silver nanoparticle/bacterial cellulose gel membranes for antibacterial wound dressing: investigation in vitro and in vivo 9 (3) (2014), 035005.
[22] T. Maneerung, S. Tokura, R.J.C.p. Rujiravanit, Impregnation of silver nanoparticles into bacterial cellulose for antimicrobial wound dressing 72 (1) (2008) 43–51.
[23] F. Ostadhossein, N. Mahmoudi, G. Morales-Cid, E. Tamjid, F.J. Navas-Martos, B. Soriano-Cuadrado, J.M.L. Paniza, A.J.M. Simchi, Development of chitosan/bacterial cellulose composite films containing nanodiamonds as a potential flexible platform for wound dressing 8 (9) (2015) 6401–6418.
[24] X. Du, L. Wu, H. Yan, Z. Jiang, S. Li, W. Li, Y. Bai, H. Wang, Z. Cheng, D.J.N. c. Kong, Microchannelled alkylated chitosan sponge to treat noncompressible hemorrhages and facilitate wound healing 12 (1) (2021) 4733.
[25] S. Torkaman, H. Rahmani, A. Ashori, S.H.M.J.C.P. Najafi, Modification of Chitosan Using Amino Acids for Wound Healing Purposes: A Review, 2021, p. 117675.
[26] S. Rashki, K. Asgarpour, H. Tarrahimofrad, M. Hashemipour, M.S. Ebrahimi, H. Fathizadeh, A. Khorshidi, H. Khan, M. Salavati-Niasari, H.J.C.P. Mirzaei, Chitosan-based Nanoparticles against Bacterial Infections, 2020, p. 117108.
[27] R. Poonguzhali, S.K. Basha, V.S.J.I.J.o.B.M. Kumari, Novel Asymmetric chitosan/PVP/nanocellulose Wound Dressing: in Vitro and in Vivo Evaluation, 2018, p. 112.
[28] S. Fernandes, B.L. Oliveira, A. Freire, A.J.G.C. Silvestre, Novel transparent nanocomposite films based on chitosan and bacterial cellulose 11 (12) (2009) 2023–2029.
[29] K.M. Pasaribu, S. Gea, S. Ilyas, T. Tamrin, I.J.B. Radecka, Characterization of bacterial cellulose-based wound dressing in different order impregnation of chitosan and collagen 10 (11) (2020) 1511.
[30] J. Xia, H. Zhang, F. Yu, Y. Pei, X.J.A.a.m. Luo, interfaces, Superclear, porous cellulose membranes with chitosan-coated nanofibers for visualized cutaneous wound healing dressing 12 (21) (2020) 24370–24379.
[31] O. Fatemeh, M. Nafiseh, M.C. Gabriel, T. Elnaz, N.M. Francisco, S. Belén, P. José, S. J.M. Abdolreza, Development of chitosan/bacterial cellulose composite films containing nanodiamonds as a potential flexible platform for wound dressing 8 (9) (2015).
[32] J. Kim, Z. Cai, H.S. Lee, G.S. Choi, D.H. Lee, C.J.J.o.P.R. Jo, Preparation and characterization of a Bacterial cellulose/Chitosan composite for potential biomedical application 18 (4) (2011) 739–744.
[33] T.T. Nge, M. Nogi, H. Yano, J.J.C. Sugiyama, Microstructure and mechanical properties of bacterial cellulose/chitosan porous scaffold 17 (2) (2010) 349–363.

[34] J. Kingkaew, S. Kirdponpattara, N. Sanchavanakit, P. Pavasant, M.J. B. Phisalaphong, B. Engineering, Effect of molecular weight of chitosan on antimicrobial properties and tissue compatibility of chitosan-impregnated bacterial cellulose films 19 (3) (2014) 534–544.
[35] M. Khamrai, S.L. Banerjee, P.P. Kundu, Modified bacterial cellulose based self-healable polyeloctrolyte film for wound dressing application, Carbohydr. Polym. 174 (2017) 580–590.
[36] L.V. Cabañas-Romero, C. Valls, S.V. Valenzuela, M.B. Roncero, F.J. Pastor, P. Diaz, J.J.B. Martínez, Bacterial cellulose–chitosan paper with antimicrobial and antioxidant activities 21 (4) (2020) 1568–1577.
[37] V. Dubey, L. Pandey, C.J.J.o.M.S. Saxena, Pervaporative separation of ethanol/water azeotrope using a novel chitosan-impregnated bacterial cellulose membrane and chitosanpoly(vinyl alcohol) blends 251 (1–2) (2005) 131–136.
[38] M. Salari, M.S. Khiabani, R.R. Mokarram, B. Ghanbarzadeh, H.S.J.C.P. Kafil, Use of gamma irradiation technology for modification of bacterial cellulose nanocrystals/chitosan nanocomposite film 253 (2021) 117144.
[39] M. Phisalaphong, N.J.C.P. Jatupaiboon, Biosynthesis and characterization of bacteria cellulose–chitosan film 74 (3) (2008) 482–488.
[40] Y.W. A, X.Y. B, K.Y. A, H.M.A. B, Y.Z. A, J.P. B, S.L. B, X.L. A, Y.X. A, K.Q.J.B. A, Fabrication of nanofibrous microcarriers mimicking extracellular matrix for functional microtissue formation and cartilage regeneration 171 (2018) 118–132.
[41] J. Wu, Y. Zheng, W. Song, J. Luan, X. Wen, Z. Wu, X. Chen, Q. Wang, S. Guo, In situ synthesis of silver-nanoparticles/bacterial cellulose composites for slow-released antimicrobial wound dressing, Carbohydr. Polym. 102 (2014) 762–771.
[42] J. Wu, Y. Zheng, Z. Yang, Q. Lin, K. Qiao, X. Chen, Influence of dialdehyde bacterial cellulose with the nonlinear elasticity and topology structure of ECM on cell adhesion and proliferation, RSC Adv. 4 (2014) 3998–4009.
[43] L. Yue, Y. Zheng, Y. Xie, S. Liu, S. Guo, B. Yang, T. Tang, Preparation of a carboxymethylated bacterial cellulose/polyaniline composite gel membrane and its characterization, RSC Adv. 6 (73) (2016) 68599–68605.
[44] Y. Lin, Q.B. Lin, Z. Jiang, W. Zhang, X.C.J.C.J. o A C C, Preparation, Moisture Adsorbability and Retentivity of 2-Hydroxypropyltrimethyl Ammonium Chloride Chitosan, 2002.
[45] X. Wang, C. You, X. Hu, Y. Zheng, Q. Li, Z. Feng, H. Sun, C. Gao, C.J.A.B. Han, The roles of knitted mesh-reinforced collagen–chitosan hybrid scaffold in the one-step repair of full-thickness skin defects in rats 9 (8) (2013) 7822–7832.
[46] S. Liu, M. Chu, Y. Zhu, L. Li, L. Wang, H. Gao, L. Ren, A novel antibacterial cellulose based biomaterial for hernia mesh applications, RSC Adv. 7 (19) (2017) 11601–11607.
[47] K. Yoshino, R. Matsuoka, K. Nogami, S. Yamanaka, K. Watanabe, M. Takahashi, M. Honma, Graphite film prepared by pyrolysis of bacterial cellulose, J. Appl. Phys. 68 (4) (1990) 1720–1725.
[48] T. Ristić, A. Zabret, L. Zemljič, Z.P.J. Cellulose, Chitosan nanoparticles as a potential drug delivery system attached to viscose cellulose fibers 24 (2) (2016) 1–15.
[49] A. Anitha, V.D. Rani, R. Krishna, V. Sreeja, N. Selvamurugan, S. Nair, H. Tamura, R. Jayakumar, Synthesis, characterization, cytotoxicity and antibacterial studies of chitosan, O-carboxymethyl and N, O-carboxymethyl chitosan nanoparticles, Carbohydr. Polym. 78 (4) (2009) 672–677.
[50] Z. Shariatinia, Carboxymethyl chitosan: properties and biomedical applications, Int. J. Biol. Macromol. 120 (2018) 1406–1419.
[51] H.Q. A, T.G. B, Y.Z. A, L.Z. B, Y.S. A, Y.L. B, Y.X.J.C.P. A, A novel microporous oxidized bacterial cellulose/arginine composite and its effect on behavior of fibroblast/endothelial cell - ScienceDirect 184 (2018) 323–332.